

Partially unzipped carbon nanotubes as magnetic field sensors

S. Costamagna,^{1,2} A. Schulz,¹ L. Covaci,¹ and F. Peeters¹

¹⁾ *Universiteit Antwerpen, Department of Physics, Groenenborgerlaan 171, 2020 Antwerpen, Belgium.*

²⁾ *Facultad de Ciencias Exactas Ingeniería y Agrimensura, Universidad Nacional de Rosario and Instituto de Física Rosario, Bv. 27 de Febrero 210 bis, 2000 Rosario, Argentina.*

(Dated: 12 November 2018)

The conductance, $G(E)$, through graphene nanoribbons (GNR) connected to a partially unzipped carbon nanotube (CNT) is studied in the presence of an external magnetic field applied parallel to the long axis of the tube by means of non-equilibrium Green's function technique. We consider (z)igzag and (a)rmchair CNTs that are partially unzipped to form aGNR/zCNT/aGNR or zGNR/aCNT/zGNR junctions. We find that the inclusion of a longitudinal magnetic field affects the electronic states only in the CNT region, leading to the suppression of the conductance at low energies. Unlike previous studies, for the zGNR/aCNT/zGNR junction in zero field, we find a sharp dip in the conductance as the energy approaches the Dirac point and we attribute this non-trivial behavior to the peculiar band dispersion of the constituent subsystems. We demonstrate that both types of junctions can be used as magnetic field sensors.

Among the existing available techniques to produce GNRs¹⁻⁴, a very appealing one is the unzipping of CNTs. This can be done, for example, by using chemical attack⁵ or thought plasma beam etching⁶. Although recent molecular dynamics studies have shown that dangling bonds tend to re-bond on partially unzipped CNT, by fully hydrogenating the opened edges this self-healing behavior can be suppressed⁷. Thus, it is feasible that multi-junctions composed of CNTs and GNRs can be fabricated in the near future. From a theoretical point of view, the electronic transport properties of such junctions have been addressed in a series of works. In Ref. 8 the conductance of partially unzipped aCNT/zGNR junctions was numerically studied. The case of unzipped zCNT was addressed in Refs. 9 and 10 where analytical expressions for the wave functions and transmission probabilities were obtained by connecting different parts of the system under proper boundary conditions. The main result is that the metallic aGNR/zCNT/aGNR junctions exhibit perfect transmission for incident low-energy electrons. Different from previous works, here we are interested to study the conductance of partially unzipped CNT in the presence of an external magnetic field parallel to the tube axis. We will analyze the aGNR/zCNT/zGNR and zGNR/aCNT/zGNR junctions schematically displayed in Fig. 1. We will show that variations in the external magnetic field can dramatically change the conductance of the system and therefore we propose to use these systems as magnetic field sensors. Such sensors have the additional advantage that much better contacts can be realized on the ribbon sections as compared to plain nanotubes.

In order to describe the electron hopping between the π orbitals pertaining to neighboring carbon atoms we adopt a nearest-neighbor tight binding Hamiltonian. The unzipped systems studied here (a) zCNT and (b) aCNT, are displayed in Fig. 1. Note that, for simplicity we have adopted a different enumeration N_x and N_y to define

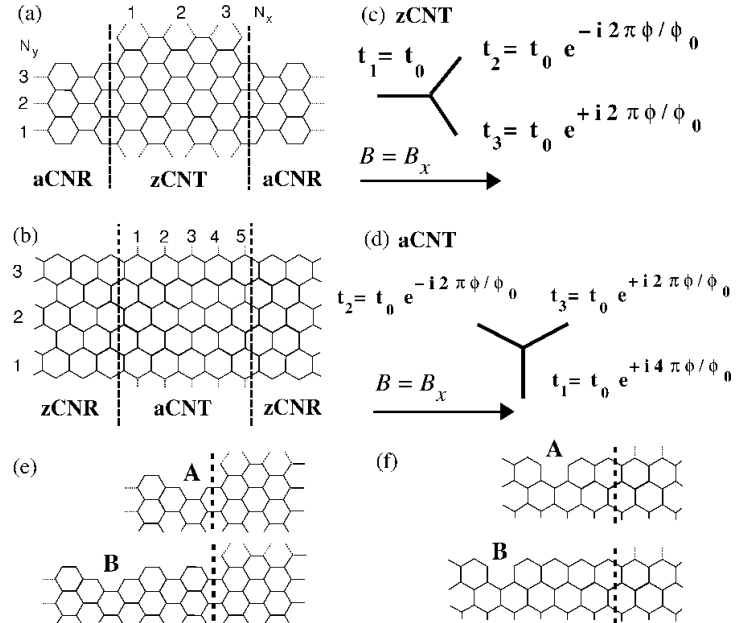


FIG. 1. (a) aGNR/zCNT/aGNR and (b) zGNR/aCNT/zGNR junctions. The dashed thick vertical lines separate each part of the system considered for the conductance calculation. The Peierls factors (c-d) modifying the hopping amplitudes in the CNTs appearing due to the magnetic fields are $\phi = Bra\sqrt{3}/2$ for the zCNT and $\phi = Bra/2$ for the zCNT. The size of the zCNT (aCNT) is defined by $N_x = 3$ and $N_y = 3$ ($N_x = 5$ and $N_y = 3$) as indicated on the plot. Edge vacancies considered in this work are displayed in (e) and (f).

each geometry and that periodic boundary condition are used at the two edges to define the tubes.

When a CNT is partially unzipped we model it as a CNT that is connected to ribbons on both of its sides. The aGNR/zCNT/aGNR system can be thought of as a zCNT from which one line of C-atom dimers is removed

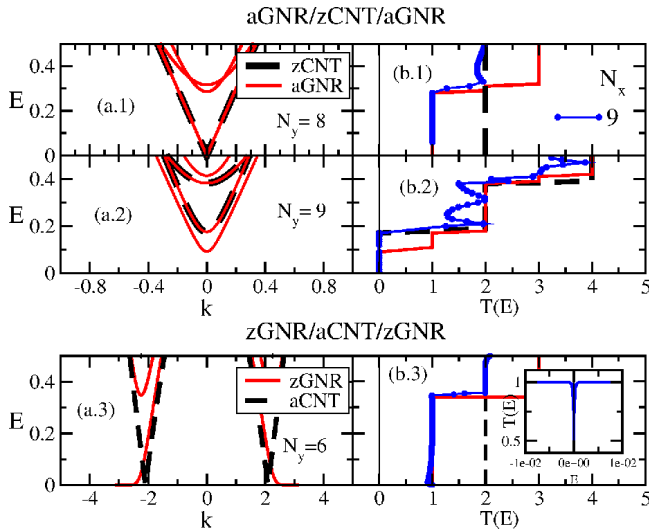


FIG. 2. (Color online)(a) Bandstructure of pure CNTs (dashed lines) and GNRs (solid lines) as indicated. $T(E)$ for each corresponding junction is shown in (b) for $N_x = 9$. $T(E)$ for the pure CNTs (dashed lines) and GNR (solid lines) were included for a better comprehension. The inset shows the vanishing of $T(E)$ at very low energies in the case of zGNR/aCNT/zGNR junctions (see text).

in the left and right section, forming the aGNR-leads. In the zGNR/aCNT/zGNR system, no atoms are removed, but the bonds between two zigzag edges are removed. In both cases the model Hamiltonian describing the whole system is therefore given by

$$H = H_{z(a)CNT} + H_{a(z)GNR_L} + H_{a(z)GNR_R} \quad (1)$$

where $H_{a(z)GNR_{L(R)}}$ corresponds to the semi-infinite left (right) lead, and $H_{z(a)CNT}$ describes the nanotube. In addition to these terms we have h_{LC} and h_{LR} which are the hopping amplitudes connecting the leads to the nanotube. The hopping parameter between carbon atoms, $t_0 = 2.7$ eV, is taken as unit of energy. The conductance calculation was done by using the non equilibrium Green's function technique^{11–13} where $G(E)$ is obtained from the transmission function $T(E)$ as $G(E) = (2e^2/h)T(E)$. We remark that the self-energies for the semi-infinite leads have been computed self-consistently and when used to calculate the $G(E)$ of pure CNTs and GNRs they give the expected value as shown in Fig. 2. Even without external magnetic field, very different low energy electronic properties can be present in these junctions. In the case of zCNTs/aGNRs, it is known that the metallicity of undoped samples is determined by the width of the tubes and ribbons.⁹ In Fig. 2, panels (a.1) and (a.2) show the low energy band-structure for pure infinitely long aGNRs and zCNTs of different widths. In both, the metallic and the semiconducting regimes, only some of the bands of the aGNR coincide with the bands of the zCNT due to the different transverse boundary conditions (open vs. periodic), see e.g.

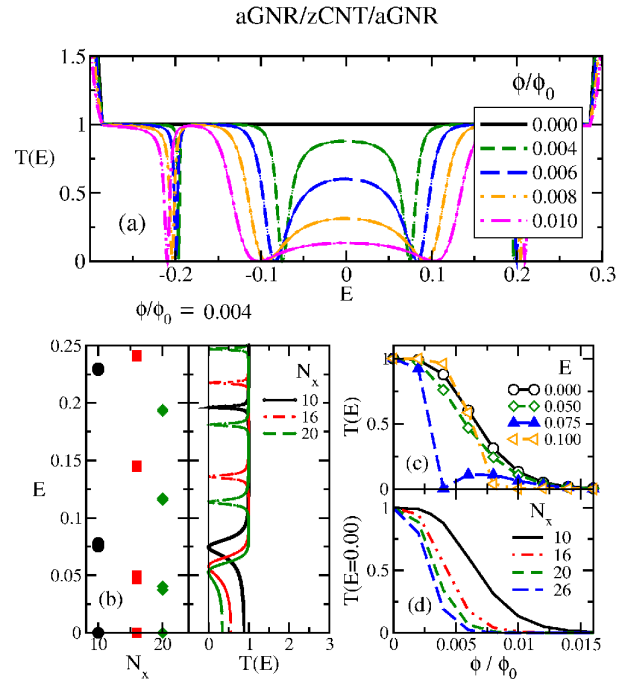


FIG. 3. (Color online) (a) $T(E)$ in the unzipped zCNT ($N_y = 8$, $N_x = 10$) for different magnetic fields. (b) Low energy spectrum of an isolated zCNT and $T(E)$ for different tube lengths. $\phi/\phi_0 = 0.004$ and $N_y = 8$ in both cases. (c) Variation of $T(E)$ for several energies near zero (extracted from (a)) and (d) decay of $T(E = 0.00)$, for several tube length as indicated, against the magnetic field.

Ref. 9. In addition, while each band of the aGNR is non-degenerate, in the zCNT the bands are doubly degenerate⁹ which implies that for low energies metallic zCNT possess a higher conductance than aGNR. For the partially unzipped aGNR/zCNT/aGNR metallic junctions, i.e. $N_y = 8$, it is expected that in the absence of the magnetic field the system should show no backscattering and a perfect conductance at low energies⁹. Accordingly we see in Fig. 2 (b.1) that the transmission remains unity at low energies. For higher energies $G(E)$ shows the expected jumps each time that a new channel is available for conduction.

On the other hand, in the case of the zGNR/aCNT/zGNR junction (Fig. 2 (a.3) and (b.3)) we observe a quite different low energy behavior. While zGNRs are always metallic independent of their width, due to the localized edge states at zero energy, $T(E)$ vanishes in the combined system when the energy approaches zero, which is made more clear in the inset of Fig. 2. This sharp drop in the conductance at zero energy can be understood from the mismatch in the dispersion of the zGNR and aCNT subsystems, (cf. Fig. 2 (a.3)), as the energy approaches zero. Due to the resulting difference in momentum of the corresponding eigenstates, electron wave-functions incident from the ribbon become evanescent in the aCNT and therefore the conduction is suppressed. Although not shown here,

we have found that this suppression is sensitive to the length of the aCNT subsystem, as the electron tunnels through it.

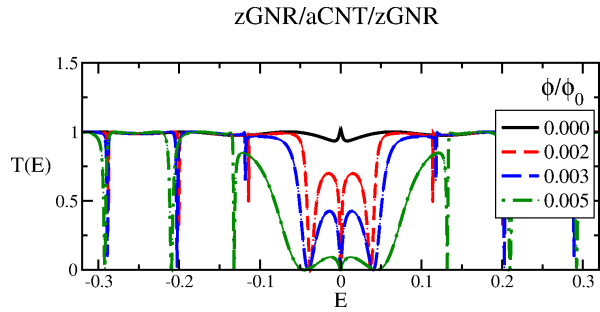


FIG. 4. (Color online) Variation of $T(E)$ in the unzipped aCNT ($N_y = 6$, $N_x = 24$) for different magnetic fields as indicated on the plot.

When an external magnetic field is acting on the CNTs it can be included into the tight binding Hamiltonian using the so-called Peierls phase from which $t_{ij} = -t_0 e^{-ie/\hbar \int_i^j \vec{A} \cdot d\vec{l}}$ where $\vec{B} = \vec{\nabla} \times \vec{A}$ and the integration is done along the hopping path. For a magnetic field parallel to the tube axis, this is $B = B_x$, there will be only three different hopping phases. These terms were displayed in Fig. 1(c) and Fig. 1(d). $\phi_0 = h/e$ is the quantum flux, r is the radius of the tube, B is the magnitude of the magnetic field and $a = 1.42\text{\AA}$ is the carbon atoms distance. For the GNR the axial magnetic field has no effect since the flux through the ribbon is zero.

The effect of the magnetic field on the aGNR/zCNT/aGNR junction is shown in Fig. 3. At low energies the transmittance is suppressed due to the magnetic field induced gap in the zCNT (this comes about because the magnetic field will shift the transverse momentum thus changing a metallic nanotube into a semiconducting one). The suppression is due to a decrease of the overlap of evanescent modes from the aGNR and depends on the tube length as can be seen in Fig. 3(b). Thus, when the transmittance vs. magnetic flux is plotted for different energies and tube lengths, as shown in Figs. 3(c-d), we notice that this junction could be used as a magnetic sensor since the resistance of the junction is very sensitive to magnetic field changes. The longer the tube length, more sensitive the sensor will be since smaller magnetic fields are needed to suppress the overlap of the wave functions coming from the leads. When the Fermi level is shifted from the Dirac point for certain energies, which depends on the tube length, the transmittance is even more sensitive to changes in the magnetic field thus improving the efficiency of the sensor. For the zGNR/aCNT/zGNR junction, the dependence of the transmittance is presented in Fig. 4. Except to the peculiar zero energy suppression, the behavior is similar to the aGNR/zCNT/aGNR junction thus making the operation of the proposed magnetic sensor independent of the orientation of the partially

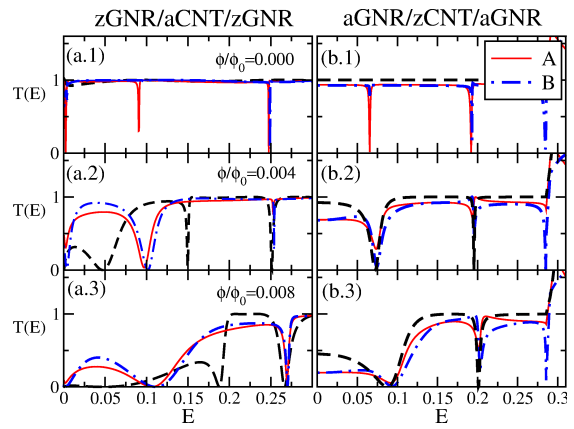


FIG. 5. (Color online) Effect of edge vacancies on $T(E)$ in the (a) zGNR/aCNT/zGNR ($N_x = 10$, $N_y = 6$) and (b) aGNR/zCNT/aGNR ($N_x = 10$, $N_y = 8$) junctions for different magnetic fields as indicated. The location of the vacancies named A and B is displayed in Figs. 1(e,f). $T(E)$ for the case where there are no vacancies is indicated by the black-dashed line.

unzipped CNTs¹⁴. The effect of defects as Carbon atoms vacancies on the edges of the ribbons, where they are more likely to appear in the unzipping process, is shown in Fig. 5. While edge defects modify the conductance, their effects can be clearly distinguished from the effects of the magnetic field and thereby the performance of these magnetic fields sensors holds.

Magnetic field induced changes of the electronic properties in the zCNT/aGNR regions will modify the magneto-resistance of the junctions which hence can be used as magnetic field sensors. While more realistic system sizes are out of the scope of the numerical technique employed, given a tube radius of $r = 500\text{nm}$, ϕ/ϕ_0 equals to 0.001 which implies a magnetic field $B \approx 0.67 - 1.16$ T depending on the junction. Therefore, the simplicity of the sensor, due to the fact that the GNRs are perfect contacts to the CNTs while the magnetic field does not affect the contacts, makes it interesting for possible applications. Edge defects in the ribbons do not modify the qualitative behavior of the junctions and their effect on the conduction can be neglected when the defects are far from the junction (e.g. farther than 1nm). Also, due to the extraordinary stiffness of CNTs, in the relaxed configuration the nanotube region is expected to be straight and therefore curvature effects can be safely neglected.

Acknowledgments LC acknowledges support from the Flemish Science Foundation (FWO-VI) and SC from the Belgian Science Foundation (BELSPO). This work is supported by the ESF-EuroGRAPHENE project CONGRAN.

REFERENCES

- ¹H. C. Schniepp, Je-Luen Li, M. J. McAllister, H. Sai, M. Herrera-Alonso, D. H. Adamson, R. K. Prud'homme, R. Car, D. A. Saville and I. A. Aksay, *J. Phys. Chem. B* **110**, 8535 (2006).
- ²X. Li, X. Wang, Li Zhang, S. Lee and H. Dai, *Science* **319**, 1229 (2008).
- ³X. Yang, Xi Dou, A. Rouhanipour, L. Zhi, H. J. Rder, and K. Mllen, *J. Am. Chem. Soc.* **130**, 4216 (2008).
- ⁴J. Cai, P. Ruffieux, R. Jaafar, M. Bieri, T. Braun, S. Blankenburg, M. Muoth, A. P. Seitsonen, M. Saleh, X. Feng, K. Mllen and R. Fasel, *Nature (London)* **466**, 470473 (2010).
- ⁵D. V. Kosynkin, A. L. Higginbotham, A. Sinitskii, J. R. Lomeda, A. Dimiev, B. K. Price, J. M. Tour, *Nature (London)* **458**, 872 (2009).
- ⁶L. Jiao, L. Zhang, X. Wang, G. Diankov, H.J. Dai, *Nature (London)* **458**, 877 (2009).
- ⁷C. Tang, W. Guo and C. Chen, *Phys. Rev. B* **83**, 075410 (2011).
- ⁸H. Santos, L. Chico, and L. Brey, *Phys. Rev. Lett.* **103**, 086801 (2009).
- ⁹Y. Klymenko and O. Shevtsov, *Eur. Phys. J. B* **72**, 2 (2009) 203-209.
- ¹⁰Yu. O. Klymenko, *Eur. Phys. J. B* **77**, 3 (2010) 433-440.
- ¹¹S. Datta, *Electronic Transport in Mesoscopic Systems* (Cambridge University Press, 1995).
- ¹²H. Xu, T. Heinzl, M. Evaldsson and I. V. Zozoulenko, *Phys. Rev. B* **77**, 245401 (2008).
- ¹³S. Costamagna, O. Hernandez and A. Dobry, *Phys. Rev. B* **81**, 115421 (2010).
- ¹⁴Although not shown here, we have found the same behavior for metallic junctions with different widths.